STATE OF OREGON
DEPARTMENT OF GEOLOGY AND MINERAL INDUSTRIES
Suite 965, 800 NE Oregon St., #28
Portland, Oregon 97232

Interpretive Map Series

IMS-16

Earthquake Scenario and Probabilistic Ground Shaking Maps for the Portland, Oregon, Metropolitan Area

By

Ivan Wong, Walter Silva, Jacqueline Bott, Douglas Wright, Patricia Thomas, Nick Gregor, Sylvia Li, Matthew Mabey, Anna Sojourner, and Yumei Wang

2000

Funded by the U.S. Geological Survey
under National Earthquake Hazards Reduction Program Award
Number 1434-HQ-96-GR-02727

Contents

Map sheets (folded, in envelope)

1. Earthquake scenario ground shaking map for the Portland, Oregon, metropolitan area, Portland Hills fault M 6.8 earthquake, 0.2 second spectral acceleration at the ground surface
2. Earthquake scenario ground shaking map for the Portland, Oregon, metropolitan area, Portland Hills fault M 6.8 earthquake, 1.0 second spectral acceleration at the ground surface
3. Earthquake scenario ground shaking map for the Portland, Oregon, metropolitan area, Cascadia subduction zone M 9.0 earthquake, peak horizontal acceleration at the ground surface
4. Earthquake scenario ground shaking map for the Portland, Oregon, metropolitan area, Cascadia subduction zone M 9.0 earthquake, 0.2 second spectral acceleration at the ground surface
5. Earthquake scenario ground shaking map for the Portland, Oregon, metropolitan area, Cascadia subduction zone M 9.0 earthquake, 1.0 second spectral acceleration at the ground surface
6. Probabilistic earthquake ground shaking map for the Portland, Oregon metropolitan area, 10% probability of exceedance in 50 years, peak horizontal acceleration at the ground surface
7. Probabilistic earthquake ground shaking map for the Portland, Oregon metropolitan area, 10% probability of exceedance in 50 years, 0.2 second spectral acceleration at the ground surface
8. Probabilistic earthquake ground shaking map for the Portland, Oregon metropolitan area, 10% probability of exceedance in 50 years, 1.0 second spectral acceleration at the ground surface
9. Probabilistic earthquake ground shaking map for the Portland, Oregon, metropolitan area, 2% probability of exceedance in 50 years, peak horizontal acceleration at the ground surface
10. Probabilistic earthquake ground shaking map for the Portland, Oregon, metropolitan area, 2% probability of exceedance in 50 years, 0.2 second spectral acceleration at the ground surface
11. Probabilistic earthquake ground shaking map for the Portland, Oregon, metropolitan area, 2% probability of exceedance in 50 years, 1.0 second spectral acceleration at the ground surface

LIMITATIONS

There are large uncertainties associated with ground motion prediction in the Pacific Northwest due to a limited amount of region-specific information and data on the characteristics of seismic sources and ground motions. In the portrayal of the Cascadia subduction zone scenario, the uncertainties in the geometry and eastward extent of the rupture are particularly large. Additional uncertainty stems from the characterization of the subsurface geology beneath Portland and the estimation of the associated site response effects on ground motions. Thus the maps should not be used for site-specific design or in place of site-specific hazard evaluations.

IMS–16

Earthquake Scenario and Probabilistic Ground Shaking Maps for the Portland, Oregon, Metropolitan Area

By

Ivan Wong[1], Walter Silva[2], Jacqueline Bott[1,4], Douglas Wright[1], Patricia Thomas[1], Nick Gregor[2], Sylvia Li[2], Matthew Mabey[3,5], Anna Sojourner[1], and Yumei Wang[3]

ABSTRACT

We have developed the first quantitative earthquake scenario and probabilistic microzonation maps for ground shaking for the Portland, Oregon, metropolitan area. These GIS-based maps display color-contoured ground motion values in terms of peak horizontal acceleration and horizontal spectral accelerations at 0.2- and 1.0-second periods. The maps depict ground shaking at the ground surface and thus incorporate the site-response effects of soils, unconsolidated sediments, and shallow rock. The scenario maps are for a moment magnitude (M_W) 9.0 earthquake along the megathrust of the Cascadia subduction zone and a hypothetical M_W 6.8 event on the Portland Hills fault. The probabilistic maps are for the two return periods of building code relevance, 500 and 2,500 years. It is our hope that these maps will be used by government agencies, the engineering, urban planning, emergency preparedness and response communities, and the general public as part of an overall effort to reduce earthquake hazards in the Portland metropolitan area.

INTRODUCTION

The Portland metropolitan area and surrounding vicinity have been the most seismically active region in Oregon in historical times. Based on the relatively brief 150-year historic record, six earthquakes of Richter magnitude (M_L) 5 or greater have occurred within the greater Portland area including the damaging M_L 5.5 Portland earthquake of 1962 and the M_L 5.6 Scott Mills earthquake of 1993 (Bott and Wong, 1993). In contrast, recent geophysical studies indicate the presence of at least three crustal faults beneath the Portland metropolitan area (Blakely and others, 1995; Pratt and others, in preparation) which could generate much more damaging crustal earthquakes of M_L 6.5 or larger. An evaluation of earthquake recurrence based on the historical record suggests that crustal earthquakes of M_L 6.5 and larger occur somewhere in the Portland region on average about every 1,000 years (Bott and Wong, 1993). Additionally, a convincing case has now been made to indicate that Cascadia subduction zone earthquakes up to moment magnitude (M_W) 9 have occurred in the prehistoric past, as recently as the year 1700, and will occur in the future (e.g., Atwater and others, 1995; Satake and others, 1996). Thus, although in its 150-year existence the Portland metropolitan area has gone relatively unscathed by damaging earthquakes, strong ground shaking generated by either a Cascadia subduction zone earthquake or a nearby crustal event will certainly have a major future impact on the Portland area.

The purpose of this study was to develop both deterministic earthquake scenario maps and probabilistic ground shaking maps at a microzonation level for the Portland metropolitan area (defined as the Portland, Mount Tabor, Gladstone, Lake Oswego, Beaverton, and Linnton quadrangles). The most up-to-date information on seismic sources, including characteris-

[1] Seismic Hazards Branch, URS Greiner Woodward Clyde Federal Services, 500 12th Street, Suite 200, Oakland, CA 94607
[2] Pacific Engineering & Analysis, 311 Pomona Avenue, El Cerrito, CA 94530
[3] Oregon Department of Geology and Mineral Industries, 800 NE Oregon Street, Portland, OR 97232
[4] Now at British Geological Survey, Edinburgh, Scotland, U.K.
[5] Now at Department of Geology, Brigham Young University, Provo, UT 84602

tics of the potential rupture plane for the Cascadia megathrust earthquake and crustal faults within the Portland region, has been incorporated into the analysis. The maps also incorporate the effects on ground shaking of (1) the near-surface geology based on downhole geologic and shear wave velocity data collected by the Oregon Department of Geology and Mineral Industries (DOGAMI) and (2) characteristics of the velocity structure and seismic attenuation (Q) in both the Oregon and Washington crust and the Cascadia subduction zone. Numerical ground motion modeling was used to develop region-specific attenuation relationships and site-amplification factors. These were used together with recent empirical attenuation relationships to compute the earthquake scenario and probabilistic ground motions.

Based on this approach, a total of 12 hazard microzonation maps have been produced. These include (1) earthquake scenario maps for a M_W 9 megathrust event along the Cascadia subduction zone and a nearby crustal earthquake of M_W 6.8 on the Portland Hills fault and (2) probabilistic maps for approximate return periods of 500 and 2,500 years (10% and 2% probability of exceedance in 50 years, respectively). The GIS-based maps display peak horizontal acceleration and horizontal spectral accelerations at periods of 0.2 and 1.0 seconds at the ground surface. The present map series (DOGAMI publication IMS–16) contains 11 of the 12 sheets. The map for peak horizontal acceleration in the Portland Hills fault earthquake scenario has been published separately as IMS–15.

These maps may be used for a variety of purposes, from very general to very technical, and by users of varying levels of technical expertise. It is to be noted, however, that the following text is a *technical* description of the approach used in the map development and of some important aspects of the resulting maps. For additional information, please see Wong and others (1998) or contact the first author.

METHODOLOGY AND INPUT TO HAZARD

Six principal tasks are contained in this study: (1) seismic source characterization; (2) definition and characterization of geologic site categories and computation of amplification factors; (3) seismic attenuation characterization; (4) scenario and probabilistic ground motion calculations; (5) map development; and (6) production of the final report and dissemination of results.

Seismic source characterization

The first step in any assessment of earthquake hazards requires a characterization of the seismic sources that will produce ground motions of engineering significance at the site or area of interest. For an earthquake scenario analysis, only the characterization of a single seismic source is required. Parameters needed are fault location, geometry, and orientation, sense of slip, and maximum magnitude (M_{max}). No recurrence rate information is used.

In a probabilistic hazard assessment, all seismic sources that can generate significant ground shaking at a site, generally within a distance of 100 to 200 km (in the western U.S.), are characterized. Two general types of seismic sources were considered in the probabilistic hazard analysis: active or seismogenic faults and areal source zones. Uncertainties (which were sometimes large) in the seismic source parameters described below were incorporated into the probabilistic seismic hazard analysis using a logic-tree approach. In this procedure, probable values of the source parameters are represented by the branches of logic trees, with probabilities representing the likelihood of the values to be correct. In general, three values for each parameter were weighted and used in the analysis. An example logic tree for the East Bank fault is shown in Figure 1. The following discussion focuses on the seismic source characterization for the probabilistic hazard analysis. The single values used in the scenario ground motion estimation are discussed in the section "Scenario ground motions."

Crustal faults

All known and suspected Quaternary crustal faults within the region bounded by latitudes 44° to 47° and longitudes 120.5° to 125° (northwestern Oregon and southwestern Washington) were characterized (Figure 2). Most of this characterization is based on the

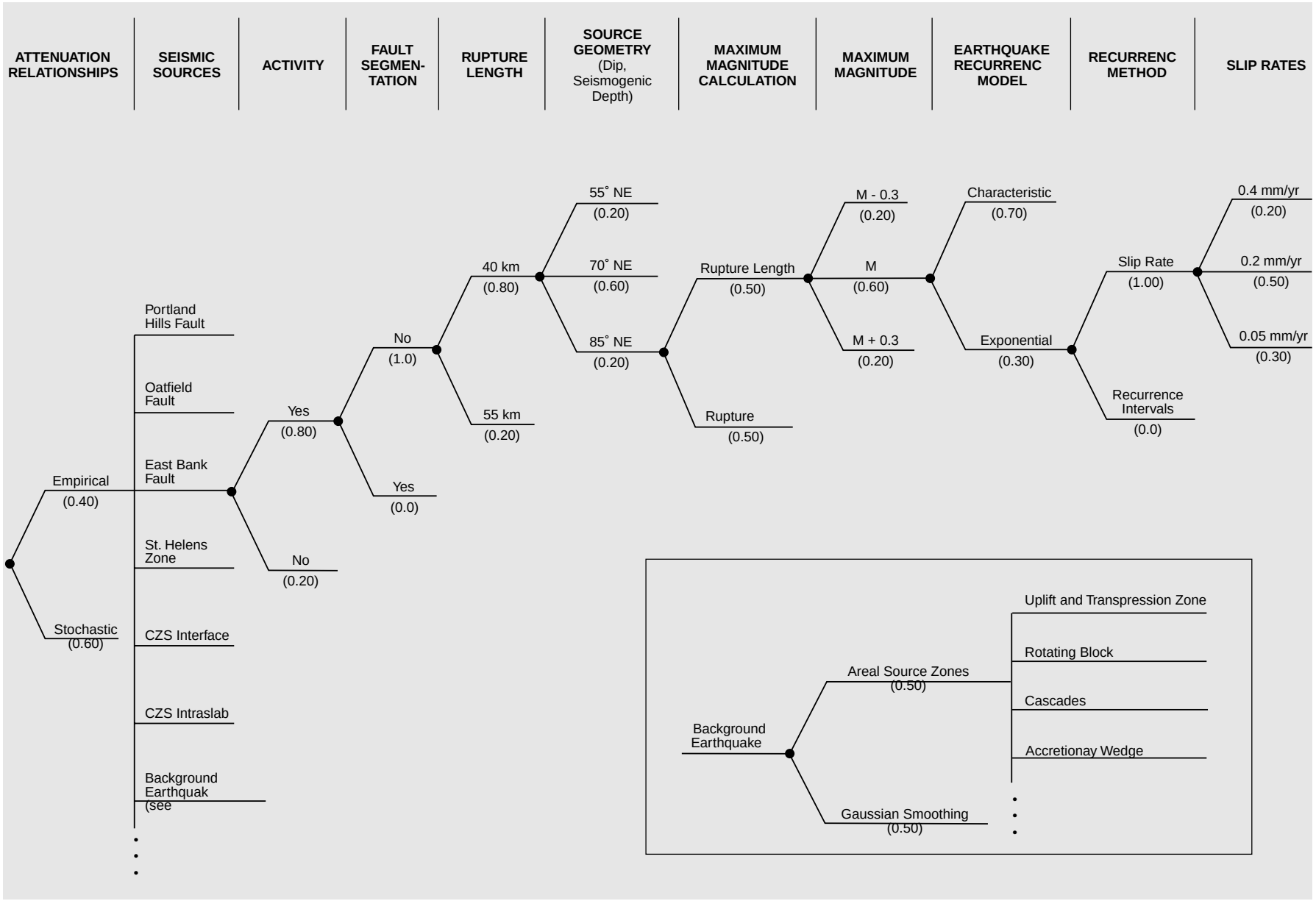

Figure 1. Example of logic tree used in seismic source characterization.

fault parameters estimated by Pezzopane (1993) and Geomatrix Consultants (1995), the latter for the Oregon Department of Transportation state seismic hazard maps. In this study, there was a total of 38 faults, including several newly recognized faults in the Portland area and southwestern Washington (Figure 2).

Fault parameters required in the probabilistic hazard analysis include (1) probability of activity; (2) fault geometry, including rupture length, rupture width, fault orientation, and sense of slip; (3) M_{max}; and (4) earthquake recurrence. Some of these parameters are shown on Table 1. Activity of a fault is defined as the probability that the fault is seismogenic. A principal criterion upon which this parameter is estimated is whether the fault has undergone displacement (generated earthquakes) in late Quaternary time (last 780,000 years).

In only a few cases, when the geologic data were available, fault rupture segments were defined (e.g., Gales Creek fault; Table 1). For most faults of any length, rupture lengths were defined as less than the total fault length, based on the assumption that it was less likely that the full length of the fault would rupture in any given event (Table 1). Rupture widths were calculated based on fault dips and by assuming that the faults extend to the base of the seismogenic

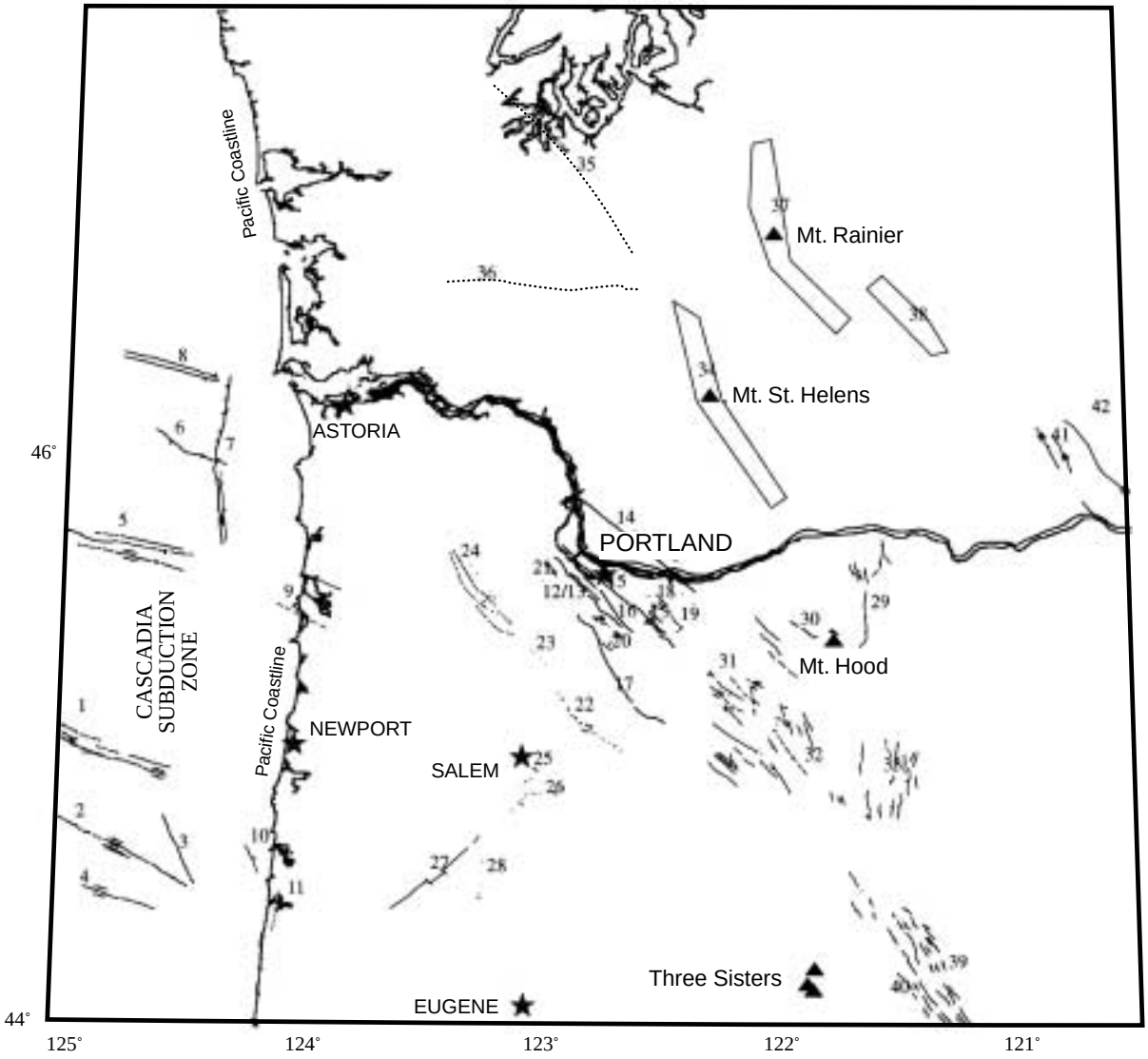

Figure 2. Quaternary faults and crustal seismic zones considered in the probabilistic seismic hazard analysis. Faults are indicated by solid lines where well located, dashed lines where uncertain or infered, and dotted where buried. Seismic zones are represented by polygons. The numbered seismic sources are keyed to Table 1.

crust—an assumption that is based on observed seismicity. For western Oregon, we assumed the seismogenic crust was either 12, 15, or 20 km thick. For the offshore region, the thicknesses were 10, 12, and 15 km. Values of 12, 15, and 18 km for seismogenic thickness were assumed for eastern Oregon. Seismogenic thicknesses were assigned weights of 0.2, 0.6, and 0.2, respectively. In the hazard analysis, fault dips were varied by ± 15° and weighted 0.2, 0.6, and 0.2, respectively (Table 1).

The magnitudes M_{max} for the faults or fault segments were calculated using the empirical relationships developed by Wells and Coppersmith (1994) between M_W and rupture length and rupture area (weighted 0.50 each). Values ranged from M_W 6.0 to 7.3 with uncertainties of ± 0.3 magnitude units (Table 1). The recurrence rates were expressed as slip rates (Table 1). The form of the recurrence model also needs to be specified. For all crustal faults, the characteristic recurrence model was weighted 0.70 and the truncated exponential model 0.30 (see Youngs and Coppersmith, 1985, for explanation of models) (Figure 1).

Of greatest significance to the hazard in Portland are the local faults, including the Portland Hills, Oatfield, East Bank, postulated Frontal (includes Lacamas Lake fault), and Mollala-Canby faults (see following section). The Oatfield, East Bank, and Mollala-Canby faults have not been previously incorporated in seismic hazard evaluations, because they were largely unknown until their delineation by Madin (1990), Beeson and others (1991), and Blakely and others (1995). No definitive evidence has been found to date that establishes the seismogenic potential of these faults, although the analyses of single seismic reflection lines across the East Bank and Portland Hills faults by Pratt and others (in preparation) have indicated possible displacements in the last 15,000 years. Contemporary seismicity has also been observed in the vicinity of the Portland Hills fault (Blakely and others, 1995).

Because of the closeness of the Portland Hills and Oatfield faults (separated by only 3–5 km) and their proposed respective westward and eastward dips, we have considered two possible structural geometries: (1) the two faults merge at a depth of 5 km and form a single zone, or (2) the two faults have steep dips and are independent structures. The scenarios were weighted 0.60 and 0.40, respectively. It is also possible that the East Bank fault may be structurally connected with the Portland Hills fault and/or the Oatfield fault, given its proximity. However, we have adopted the model proposed by Blakely and others (1995), where the East Bank fault dips away to the east, and thus have not considered this possibility in the probabilistic hazard analysis.

Slip rates of the local faults have been estimated by Wong and others (1999) based on (1) comparison of geomorphic expression with faults in other regions; (2) preliminary estimates of long-term slip rates for the Gales Creek and Mount Angel faults (R. Wells, USGS, oral communication, 1999); (3) historical seismicity; and (4) estimated range of displacements by Pratt and others (in preparation). To constrain the maximum slip-rate values shown on Table 1, Wong and others (1999) used the convergence rate of 4 to 7 mm/yr proposed by Wells and others (1998) for the Oregon forearc (western Oregon).

Cascadia subduction zone

Both the intraslab and megathrust sources of the Cascadia subduction zone were characterized (Table 2). We have adopted the Geomatrix Consultants (1995) characterization of the two intraslab sources that impact the hazard in Portland: the portion of the subducting plate beneath southwest Washington-northwest Oregon and the portion beneath central-southern Oregon region. Because there is considerable uncertainty regarding the seismogenic potential of the latter (Ludwin and others, 1991; Wong, 1997), a probability of activity of only 0.80 was assigned to this source region (Table 2). The intraslab regions were modeled as six staircasing blocks 10 km thick and 17.5 km wide, extending between the depths of 40 and 70 km as consistent with observations of intraslab seismicity in the Seattle region (Ludwin and others, 1991). A M_{max} of M_W 7.2 ± 0.3 was assumed for both intraslab zones. Recurrence parameters (Gutenberg-Richter a- and b- values) for the intraslab regions were based on the historical earthquake record. A truncated exponential model was assumed.

Table 1. Crustal fault and seismic zone parameters

Fault	Fault no.	Probability of activity	Total length (km)	Dip	Rupture length (km)	M_{max} (M_W)	Slip rate(mm/yr)
Offshore Oregon							
Wecoma fault	1	0.05	96	90°	45 (0.4), 70 (0.5), 96 (0.1)	6.8–7.2	6.5 (0.3), 8.5 (0.5), 10.5 (0.2)
Daisy Bank fault	2	0.05	98	90°	40 (0.4), 69 (0.5), 98 (0.1)	6.7–7.2	3.7 (0.3), 5.7 (0.5), 7.7 (0.2)
Stonewall Bank fault*	3	1.0	25	70°NE	25 (1.0)	6.6–6.7	0.4 (0.2), 0.9 (0.6), 1.3 (0.2)
Alvin Canyon fault	4	0.05	70	90°	27 (0.8), 70 (0.2)	6.5–7.1	4.2 (0.3), 6.2 (0.5), 8.2 (0.2)
Fault G	5	0.05	45	90°	36 (0.5), 45 (0.5)	6.7–6.9	1.0 (0.3), 5.0 (0.5), 8.0 (0.2)
Fault H	6	0.05	27	90°	15 (0.5), 27 (0.5)	6.3–6.7	1.0 (0.3), 5.0 (0.5), 8.0 (0.2)
Nehalem Bank fault	7	0.30	65	90°	37 (0.7), 65 (0.3)	6.7–7.1	0.5 (0.3), 2.0 (0.5), 5.0 (0.2)
Fault J	8	0.05	33	90°	17 (0.6), 33 (0.4)	6.3–6.8	1.0 (0.3), 5.0 (0.5), 8.0 (0.2)
Northern Coast Range							
Netarts Bay fault (Happy Camp fault)	9	0.1	20	30°N	10 (0.5), 20 (0.5)	6.3–6.8	0.005 (0.3), 0.01 (0.4), 0.04 (0.3)
Yaquina Bay fault (inferred blind thrust)	10	0.1	20	60°N	10 (0.8), 15 (0.2)	6.0–6.5	0.1 (0.2), 0.3 (0.3), 0.6 (0.5)
Waldport faults	11	0.5	14	60°E	14 (1.0)	6.3–6.5	0.05 (0.6), 0.1 (0.4)
Portland region							
Portland Hills fault**	12	0.8	62	70°SW–90°	28 (0.5), 40 (0.4), 62 (0.1)	6.6–7.1	0.05 (0.3), 0.2 (0.5), 0.4 (0.2)
Frontal Fault Zone (includes Lacamas Lake Fault)**	14	0.2 0.5	44	70°SW	21 (N) (0.8), 23 (LL) (0.8), 44 (0.2)	6.5–6.6	0.05 (0.3), 0.1 (0.4), 0.2 (0.3)
East Bank Fault*	15	0.8	55	70°NE–90°	40 (0.8), 55 (0.2)	6.8–7.1	0.05 (0.3), 0.2 (0.5), 0.4 (0.2)
Oatfield Fault*	16	0.8	40	70°NE	20 (N) (0.8), 20 (S) (0.8), 40 (0.2)	6.5–6.9	0.05 (0.3), 0.2 (0.5), 0.4 (0.2)
Mollala-Canby Fault*	17	0.5	51	70°NE	20 (0.4), 40 (0.5), 51 (0.1)	6.5–7.1	0.05 (0.3), 0.1 (0.4), 0.2 (0.3)
Sandy River Fault	18	0.1	12	70°SW	12 (1.0)	6.3–6.4	0.01 (0.4), 0.05 (0.4), 0.1 (0.2)
Grant Butte, Damascus-Tickle Creek Fault Zone	19	0.5	17	90°	10 (0.5), 17 (0.5)	6.2–6.5	0.01 (0.2), 0.05 (0.6), 0.1 (0.2)
Bolton Fault	20	0.2	9	70°N	9 (1.0)	6.1–6.3	0.005 (0.3), 0.01 (0.5), 0.05 (0.2)
Helvetia Fault	21	0.2	10	70°W	10 (1.0)	6.2–6.3	0.005 (0.3), 0.01 (0.5), 0.05 (0.2)
Mount Angel Fault**	22	0.9	32	70°NE	24 (0.5), 32 (0.5)	6.4–6.8	0.1 (0.3), 0.2 (0.4), 0.4 (0.3)
Model A [0.95]							
Newberg Fault**	23	0.7	8	70°SW	8 (1.0)	6.1–6.2	0.1 (0.3), 0.2 (0.4), 0.4 (0.3)
Model A [0.95]							
Gales Creek Fault**	24a	0.7	31	70°NE	15 (0.5), 31 (0.5)	6.4–6.8	0.1 (0.3), 0.2 (0.4), 0.4 (0.3)
Model A [0.95]							
Gales Creek-Newberg-Mt. Angel Fault Zone**	24b	0.7	90	90°	24 (0.3), 32 (0.3), 50 (0.4)	6.5–7.0	0.1 (0.3), 0.2 (0.4), 0.4 (0.3)
Model B [0.05]							
Southern Willamette Valley							
Salem Hills Structures-Waldo Hills Fault	25	0.3	25	70°NW	11 (0.5), 25 (0.5)	6.2–6.7	0.005 (0.3), 0.01 (0.5), 0.05 (0.2)
Model A [0.9]							
Mill Creek Fault	26	0.3	20	70°SE	20 (1.0)	6.5–6.6	0.005 (0.3), 0.01 (0.5), 0.05 (0.2)
Corvallis Fault	27a	0.3	41	70°SE	23 (0.4), 35 (0.4), 41 (0.2)	6.5–7.0	0.005 (0.3), 0.01 (0.5), 0.05 (0.2)
Model A [0.9]							
Corvallis-Waldo Hills Fault	27b	0.3	93	90°	11 (0.3), 25 (0.4), 41 (0.3)	6.2–6.7	0.005 (0.3), 0.01 (0.5), 0.05 (0.2)
Model B [0.1]							
Owl Creek Fault	28	0.3	15	60°SE	15 (1.0)	6.4–6.5	0.005 (0.3), 0.01 (0.5), 0.05 (0.2)
Northern Cascades							
Hood River Faults	29	0.2	47	70°W	10 (0.5), 19 (0.4), 28 (0.1)	6.2–6.7	0.05 (0.6), 0.1 (0.3), 0.2 (0.1)
Mount Hood Fault	30	0.8	21	60°NE	13 (0.7), 21 (0.3)	6.3–6.6	0.16[2] (1.0)
Clackamas River Fault Zone	31	0.5	22	70°NE	11 (0.5), 22 (0.5)	6.2–6.7	0.1 (0.3), 0.2 (0.4), 0.4 (0.3)
Model A [0.8]							
Oak Grove-Lake Harriet Fault Zone	32a	0.5	25	70°NE	10 (0.6), 20 (0.4)	6.2–6.6	0.1 (0.3), 0.2 (0.4), 0.4 (0.3)
Model A [0.8]							
Clackamas River Fault Zone-Oak Grove-Lake Harriet Fault Zone	32b	0.5	47	70°NE	11 (0.4), 22 (0.4), 47 (0.2)	6.9–7.0	0.1 (0.3), 0.2 (0.4), 0.4 (0.3)
Model B [0.2]							
Warm Springs Fault Zone-Shitike Creek Faults	33	0.4	30	70°W	17 (0.8), 30 (0.2)	6.4–6.8	0.005 (0.3), 0.01 (0.5), 0.05 (0.2)

Table 1. Crustal fault and seismic zone parameters (continued)

Fault	Fault no.	Probability of activity	Total length (km)	Dip	Rupture length (km)	M_{max} (M_W)	Slip rate(mm/yr)
St. Helens Fault Zone, WA	34	1.0	90	90°	60	5.5–6.5	Seismicity rate
Olympia Fault, WA*	35	0.5	80	70°NE	20 (0.3), 40 (0.4), 80 (0.3)	6.5–7.3	0.01 (0.3), 0.1 (0.5), 0.3 (0.2)
Doty Fault, WA*	36	0.5	65	70°N	30 (0.8), 65 (0.2)	6.7–7.2	0.01 (0.3), 0.1 (0.5), 0.3 (0.2)
Western Rainier Zone, WA*	37	1.0	90	90°	60	5.5–6.5	Seismicity rate
Goat Rocks Zone, WA*	38	1.0	33	90°	33	5.5–6.5	Seismicity Rate
Southern Cascades							
Sisters Fault Zone	39	0.9	83	90°[1]	15 (0.4), 20 (0.5), 60 (0.1)	6.3–7.1	0.01 (0.3), 0.05 (0.5), 0.1 (0.2)
Tumalo-Rimrock-Black Butte Faults	40	0.9	62	75°SW	20 (0.6), 40 (0.4)	6.5–6.9	0.01 (0.3), 0.05 (0.5), 0.1 (0.2)
Yakima Fold Belt							
Oak Flat-Luna Butte Faults, WA	41	0.5	40	90°[1]	17 (0.7), 40 (0.3)	6.4–6.9	0.01 (0.3), 0.05 (0.5), 0.1 (0.2)
Arlington-Shutler Buttes Fault Zone, OR-WA	42	0.5	70	90°[1]	25 (0.4), 45 (0.4), 70 (0.2)	6.6–7.1	0.01 (0.3), 0.05 (0.5), 0.1 (0.2)

[1] Faults within zone are steeply dipping and exhibit both down-to-the-east and down-to-the-west displacement. In the hazard analysis, they are modeled as vertical.
[2] Slip rate calculated from seismicity rate.
* Fault not considered in ODOT study.
** Values revised from ODOT study.

For the megathrust, M_{max} values of M_W 8.25, 8.5, and 9 were considered in the probabilistic analysis (Table 2). The highest weight was assigned to the M_W 9, based on the sizes of the 1700 earthquake (Satake and others, 1996) and previous events (B. Atwater, USGS, oral communication, 1997). Three scenarios for the eastern extent of the megathrust rupture were considered in the probabilistic analysis: (1) halfway into the transition zone of the Hyndman and Wang (1995) model for the Cascadia subduction zone (Wong and Silva, 1998); (2) beneath the Coast Ranges, based on paleoseismic data on coastal subsidence (Peterson and Darienzo, 1996), seismicity data (Wong, 1997), and very preliminary modeling of geodetic data by Goldfinger and others (1999); and (3) beneath the Oregon coast, representing an intermediate position between scenarios 1 and 2. The corresponding rupture widths for these three scenarios were 75, 150, and 115 km (Table 2). Scenario 3 was assigned the highest weight (0.50). Based on each of the widths, a rupture length was defined corresponding to one of the three M_{max} values (Table 2). A constant dip of 10° was assumed for the rupture plane with its top at the western edge near the deformation front at a depth of 5 km. Recurrence intervals of 450 ± 200 years (Table 2) were provided by Brian Atwater (USGS, oral communication, 1997). The characteristic model and maximum moment recurrence model (Wesnousky, 1986), weighted 0.60 and 0.40, respectively, were used for the megathrust.

Crustal seismic zones

Areal source zones are used to represent areas of observed seismicity or multiple faults. The boundaries of areal zones are often defined based on patterns of observed seismicity or tectonic/seismotectonic characteristics. In its most usual form, an areal zone is used to represent background (or random) seismicity which is associated with unknown (buried) faults.

Areal zones were used to represent three areas of localized seismicity in southwestern Washington: St. Helens (Weaver and Smith, 1983), western Rainier, and Goat Rocks seismic zones (Stanley and others, 1996) (Figure 2). The historical seismicity record (see below) was used to assess the activity rates of these zones. We assumed M_{max} values of M_W 6 ± .5 for all three zones as suggested by Weaver and Smith (1983) for the St. Helens zone.

Background seismicity

A traditional seismotectonic province approach using areal source zones (assuming uniformly distributed seismicity) and Gaussian smoothing was used to address the hazard from background earthquakes in

Table 2. Cascadia subduction zone parameters

Fault	Probability of activity	Rupture width (km)	Rupture length (km)	M_{max} (M_W)	Recurrence interval (yrs)
Megathrust	1.0	75 (0.20), 115 (0.50), 150 (0.30)	125–250	8.25 (0.25)	250 (0.3), 450 (0.4), 650 (0.3)
			225–450	8.5 (0.25)	250 (0.3), 450 (0.4), 650 (0.3)
			700–1000	9.0 (0.50)	250 (0.3), 450 (0.4), 650 (0.3)

Fault	Probability of activity	Depth range (km)	M_{max} (M_W)	Recurrence interval (yrs)
SW Washington-NW Oregon intraslab	1.0	40–70	7.0 (0.30), 7.20 (0.40), 7.5 (0.30)	Seismicity rate
Central and southern Oregon intraslab	0.8	40–70	7.0 (0.30), 7.20 (0.40), 7.5 (0.30)	Seismicity rate

the probabilistic analysis (Figures 1 and 3). Both approaches were based on a historical catalogue of the study region from 1850 to 1996 (Figure 3), which was compiled and treated for incompleteness. Dependent events were removed, uniform Richter magnitudes (assumed equivalent to M_W) were assigned, and recurrence parameters were calculated for the seismotectonic provinces. The crustal block model of Wells and others (1998) was used to define five seismotectonic provinces within the study region: rotating block, uplift and transpression zone, Cascades, fold and thrust belt, and accretionary wedge (Figure 3). We assigned M_{max} values to the provinces of M_W 6.75, 6.75, 6.25, 6.5, and 6 .5, respectively, based on our estimates of the threshold of surface faulting and seismogenic crustal thicknesses. An epistemic uncertainty of ± 0.3 magnitude units was also assumed for M_{max}. Ranges in seismogenic thickness were assigned to each seismotectonic province similar to values used for the crustal faults.

In the Gaussian filter approach (Frankel, 1995), we smoothed the treated historical background seismicity to incorporate a degree of stationarity, using a spatial window of 15 km. Because we believe the historical record may be a fairly good indicator of the distribution of background earthquakes in the next few decades, we weighted the Gaussian smoothing approach 0.70, while the seismotechnic province approach was weighted 0.30.

Geologic site categories and amplification factors

DOGAMI has developed a three-dimensional subsurface geologic model of the Portland metropolitan area that includes unconsolidated stratigraphic layer thicknesses and shear-wave velocities (Mabey and Madin, 1993). Using this model, we defined geologic site categories based on the surficial unit and the total thicknesses of all unconsolidated units above bedrock which was defined as Columbia River basalt (Tcr) or, in some locales, Boring lava (Qtb). The surficial units included the Troutdale conglomerate (Qtg), Sandy River mudstone (QTs), flood deposits of silt (Qff) and coarse-grained deposits (Qfc), loess (Qph), alluvium (Qal), and fill (Qaf). The units Qph/Qff and Qal/Qaf were combined because of their similar shear-wave velocities. Thickness ranges used were 3.0–15.2 m (10–50 ft), 15.2–30.5 m (50–100 ft), 30.5–61.0 m (100–200 ft), 61.0–121.9 m (200–400 ft), and >121.9 m (>400 ft). Units with thicknesses less than 3 m were considered to be equivalent to rock. Thus, for five surficial categories and five thickness ranges, 25 site categories were defined.

Each category was characterized by an average shear-wave velocity profile (Figure 4). Based on this profile, 30 randomized profiles were computed to account for the horizontal and vertical variability in velocities, and these were used in the simulations. Shear modulus reduction and damping curves for cohesionless soils developed by Silva and others (1997) were assigned to the various site categories to account for strain-dependent, non-linear soil response.

Based on the site category profiles and degradation curves, amplification factors were calculated. The stochastic numerical ground modeling approach coupled with an equivalent-linear methodology (Silva and oth-

ers, 1998) was used to calculate amplification factors for 5-percent-damped response spectra for each site category relative to Tcr. The point-source stochastic methodology was used to generate rock acceleration response spectra for an M_W 6.5 earthquake, which were then propagated up through the site category profiles. The M_W 6.5 event was placed at several distances to produce input peak accelerations of 0.05, 0.10, 0.20, 0.40, 0.75, and 1.25 *g*. Thus the amplification factors (the ratios of the spectra at the top of the profiles to the input spectra) are strongly a function of the reference rock peak acceleration, spectral frequency, and nonlinear soil response. Interpolation was used to obtain amplification factors at other reference rock peak accelerations. At peak horizontal acceleration, the amplification factors ranged from 0.50 to 1.42. (Factors less than 1.0 indicate deamplification relative to Tcr). At 0.2- and 1.0-second spectral accelerations, the factors ranged from 0.50 to 1.75 and 0.64 to 2.15, respectively. The velocity contrast between the low-velocity unconsolidated units and the relatively high-velocity Tcr often resulted in significant amplification particularly for thin layers of sedimentary deposits (less than 30 m thick).

Seismic attenuation characterization

Traditionally, empirical attenuation relationships for peak acceleration and response spectral values have been used to estimate ground motions. Empirical crustal relationships used in our analyses included Boore and others (1997), Abrahamson and Silva (1997), Campbell (1997), and Sadigh and others (1997). The subduction zone relationships of Youngs and others (1997)

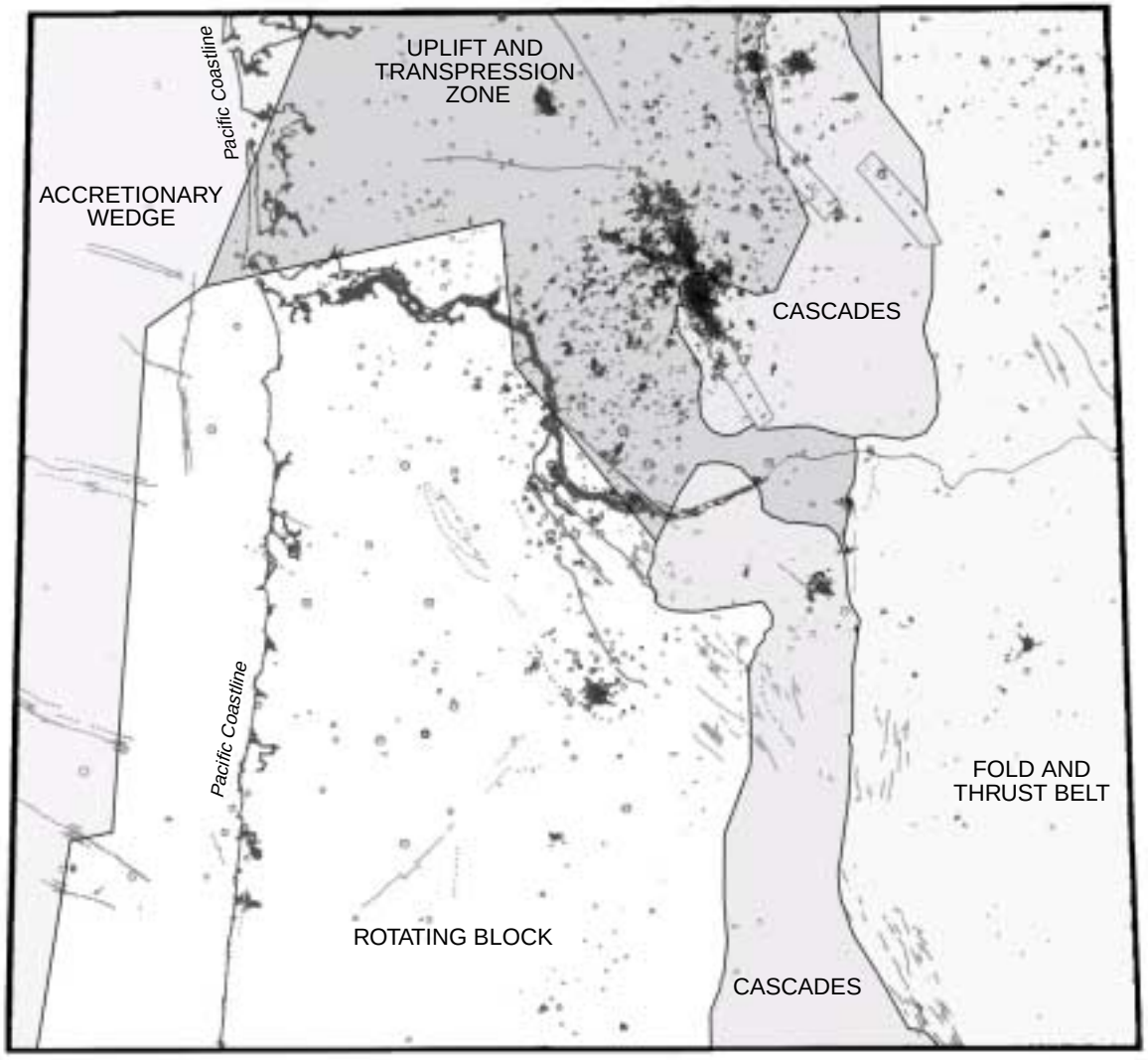

Figure 3. Seismotectonic provinces and historical seismicity, 1850 to 1996, used in the probabilistic analysis.

were used for the megathrust and intraslab sources. These empirical attenuation relationships are not region-specific because few strong-motion records exist for the Pacific Northwest (Wong, 1997).

To compensate for the lack of region-specific attenuation relationships, the stochastic ground motion modeling approach was used to develop such relationships (Wong and others, 1996) for both crustal earthquakes and the Cascadia subduction zone megathrust in the probabilistic hazard analysis. The point source version of the stochastic methodology was used to model crustal earthquakes of M_W 5.5, 6.5, and 7.5 in the distance range of 1–400 km. For the megathrust, the finite fault version was used for M_W 8, 8.5, and 9 events. Uncertainties in slip model and nucleation point (finite fault only), stress drop and magnitude-dependent focal depth (point source only), the crustal attenuation parameters Q_0 and η, and rock site parameters are included in the computations of the attenuation relationships through parametric variations (Wong and others, 1996). Uncertainties in the regression of the simulated data is added to the modeling uncertainty to produce 16th-, 50th- (median), and 84th-percentile attenuation relationships. For each magnitude and distance, 30 simulations were made and the results fitted with a functional form that accommodates magnitude-dependent saturation and far-field falloff.

Parameters for crustal attenuation as well as attenuation within the Cascadia subduction zone were adopted from Atkinson (1995). A crustal model used in the stochastic modeling was developed in this study based on the models of Trehu and others (1994), Cohee and others (1991), and Ludwin and others (1991). At the top of the crustal velocity model was Tcr, which was modeled with a relatively steep shear-wave velocity gradient in the top 60 m. At 60-m depth, the velocity was about 1,400 m/s.

Tcr was assumed to have relatively low near-surface attenuation as characterized by the parameter κ (Silva and others, 1998). A value of 0.01 s was assigned to Tcr, typical of fairly high-velocity volcanic rocks. Such low-κ rock does not significantly dampen out high-frequency ground motions as is usually observed in the typical soft rock in the western United States (Silva and Darragh, 1993). As a result, high-frequency ground motions will be higher in areas underlain by Tcr, such as the Portland metropolitan area, than in areas underlain by sedimentary rock.

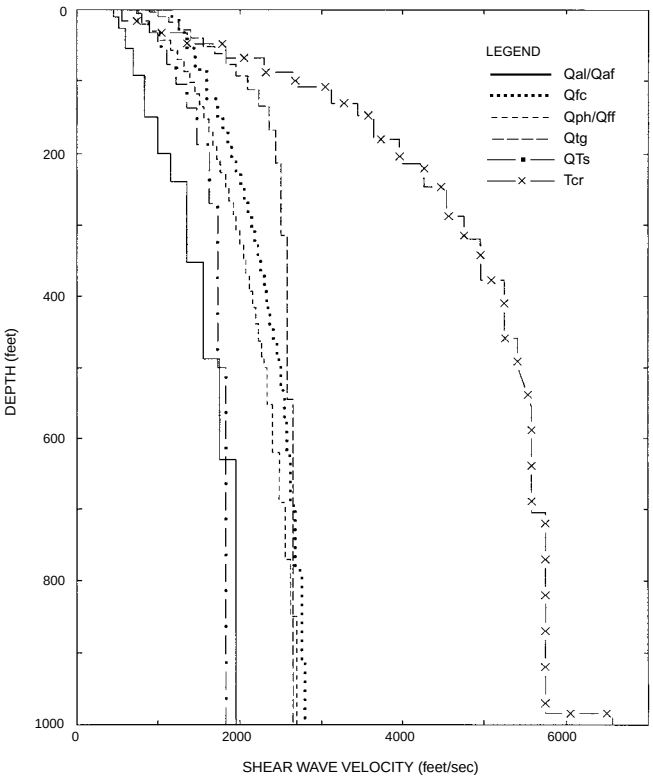

Figure 4. Average shear-wave profile for the five surficial categories and Tcr.

GROUND MOTION CALCULATIONS AND MAP DEVELOPMENT

Ground motions were estimated for both the scenario maps and the probabilistic hazard maps. Peak horizontal acceleration and spectral accelerations at spectral periods of 0.2 and 1.0 s were calculated using both empirical attenuation relationships and stochastic modeling. The resulting ground motion values were then displayed in map form using GIS.

Scenario ground motions

Ground motions were calculated for the two scenario earthquakes. The stochastic finite fault approach was used to calculate ground motions at the top of Tcr. This modeling explicitly incorporates the effects of the seismic source (fault geometry and dip, depth of rupture initiation, and sense of slip) and rupture propagation

(e.g., directivity), which are particularly important in the near field. A total of 30 simulations were made where the slip models and rupture initation were varied. The same values of Q_0 and η, assumed for the stochastic attenuation relationships were used in the scenario calculations. Scenario ground motion values were calculated for a grid of cells (see below) by assigning a 0.40 weight to the empirical values and a 0.60 weight to the numerically modeled values.

Portland Hills fault earthquake

Although the Portland Hills fault may extend for a total distance of 62 km (Figure 2), the modeled plane was assumed to coincide with the mapped trace of the fault, because this portion of the fault is the most likely site of past ruptures, based on its geomorphic expression. Thus the rupture plane for the Portland Hills fault scenario earthquake was modeled as being 30 km long, 20 km wide, and dipping 70° to the southwest. These rupture dimensions correspond to a M_W 6.8 earthquake. The sense of slip for the fault was assumed to be oblique left-lateral. As treated explicitly in the probabilistic analysis, there are numerous uncertainties in the characterization of a scenario earthquake for the Portland Hills fault, and thus the resulting ground motions may have large uncertainties. It must be emphasized that there is a small probability that the Portland Hills fault is not seismogenic (Table 1).

Cascadia subduction zone megathrust earthquake

The megathrust along the Cascadia subduction zone was modeled as being 1,000 km long, 115 km wide, and dipping 10° to the east. The eastern edge of the rupture plane of the megathrust was placed beneath the Oregon coast, which locates it about 85 km from Portland. The top of the fault was placed at a depth of 5 km and the bottom at a depth of 26 km. The uncertainties of this scenario are even greater than they are for the Portland Hills fault event. In particular, possibly the greatest uncertainty is the distance to the megathrust rupture. Dramatic increases in ground motions could result if the eastern rupture edge were moved inland.

Probabilistic ground motions

To calculate the probabilistic ground motions, a comprehensive Cornell-McGuire hazard analysis using logic trees (Figure 1) was performed, employing the computer code HAZ20 written by Norm Abrahamson. The seismic sources previously characterized were incorporated into the probabilistic analysis, and both empirical and stochastic attenuation relationships, weighted 0.4. and 0.60, respectively, were used in the analysis to calculate a mean ground motion value at the top of Tcr. The mean probabilistic hazard was calculated for peak horizontal acceleration and 0.2- and 1.0-second spectral accelerations at the two return periods of 500 and 2,500 years.

Map development

The ground shaking maps were produced using a vector- and raster-based GIS. The map area was subdivided into a raster of 880 elements or cells in which data are encoded. A cell of about 1×1 km in size was used. Each cell is represented by a point at its center, and these points were generally uniformly spaced. No point was defined whose cell crosses a lithologic boundary, so each cell could be optimally associated with a specific geologic site category. Once the cells were assigned to geologic site categories, the surface ground motions at each point were calculated by multiplying the scenario or probabilistic ground motions defined at the top of Tcr by the appropriate amplification factors. For each map, the peak or spectral acceleration values were color-contoured by interpolation in intervals of 0.05 or 0.10 *g*. The ground motion values were also spatially smoothed with a circular window of 500 m radius so that no features resulting from the contouring smaller than the grid spacing of 1 km were present on the maps. The intent was to avoid implying a level of resolution and / or accuracy that was not reasonable.

MAPS AND RESULTS

IMS-15 and sheets 1–11 in this publication, IMS–16, are the resulting hazard maps. The base map for the plates was provided by METRO from Madin (1990) and METRO's Regional Land Information System. The seismogenic faults shown are adopted from Madin (1990)

and Blakely and others (1995). To assist the layperson unfamiliar with the mapped ground motion parameters, specifically peak horizontal ground acceleration, we show a correlation between it and Modified Mercalli intensities developed by Wald and others (1999) on both the maps and in Table 3.

It must be emphasized that the ground motion values displayed on these maps may have uncertainties as large as a factor of two or more. These uncertainties reflect the current state of the art in ground motion estimation as reflected, for example, in the typical scatter of strong-motion data about a median attenuation relationship (see Abrahamson and Shedlock, 1997). Also, topographic and basin effects on ground motions have not been addressed in our analyses, although we do not believe the latter is significant because of the shallow nature of the Portland basin. Basin effects are also long-period in nature; and at 1.0-second spectral acceleration, the longest period displayed on the hazard maps, the effect, should it exist, would be minimal. It must also be noted that the mapped ground-motion values should not be used in lieu of developing site-specific seismic design criteria as specified in the Oregon Structural Specialty Code.

The following are brief general descriptions of the hazard maps.

Portland Hills fault M_W 6.8 scenario maps

The highest ground motions expected to occur in the Portland metropolitan area will be the result of rupture along one of the local crustal faults (Wong and Silva, 1998). The scenario map for the M_W 6.8 earthquake along the Portland Hills fault zone (IMS-15) illustrates this quite well. Peak horizontal accelerations may exceed 1 *g*.

IMS-15 indicates that the strongest shaking will be in the hanging wall of the fault (southwest of the fault and within about 5 km of its surface trace) as would be expected, based on theoretical radiation patterns. The maximum shaking in the Portland Hills is due to its hanging wall location and because the overlying thin (<15 m) Qph causes the greatest high-frequency site amplification anywhere in the metropolitan area at high ground motion levels (about 0.75 *g*). High-frequency ground shaking will be lower in the footwall (east of the fault) due to site damping (IMS–15). The relatively rapid decay of ground shaking to the northeast of the fault in the footwall, compared to the hanging wall, is consistent with empirical data and the physics of wave propagation. The relatively low peak accelerations along the Columbia River reflect the damping of high-frequency ground motions in the thick Qal deposits (IMS–15). A similar pattern for 0.2-second spectral acceleration is shown on Sheet 1 of IMS–16, although the site response effects on ground motions are more pronounced for this ground motion parameter because of the wide range in spectral accelerations, from 0.3 to 3.0 *g*.

At long-period ground motions (e.g., 1.0-second spectral acceleration), a somewhat contrasting pattern of ground motions is shown on Sheet 2 of IMS–16. The highest motions are either along the portion of the Portland Hills fault east of the Willamette River and away from the Portland Hills or in downtown Portland, due to moderate long-period site amplification. Some long-period amplification is also occurring in Beaverton in the Tualatin Basin (Sheet 2). In the Portland Hills, long-period ground motions, despite occurring in the hanging wall, are lower because they are not being amplified by the thin Qph deposits.

Cascadia subduction zone M_W 9.0 scenario maps

Because of the long distance to the rupture of the Cascadia subduction zone megathrust (≥85 km), high-frequency ground shaking, as depicted by peak acceleration, is relatively moderate though still strong (>0.1 *g*) and uniform across the Portland metropolitan area (Sheet 3). Site effects do not vary significantly in the metropolitan area at these ground motion levels. In general, the western half of the Portland area has the higher ground motions, being closer to the megathrust. At 0.2-second spectral acceleration, the ground motion amplitudes are naturally higher, and site amplification is more prominent particularly in the Portland Hills (Sheet 4). At 1.0-second spectral acceleration, the long-period ground motions from the M_W 9.0 subduction zone earthquake are amplified at deep Qal sites along the Columbia River and portions of the Willamette

Table 3. Relationship of peak horizontal ground acceleration (PGA) to Modified Mercalli (MM) intensity (adopted from Wald and others, 1999)

MM intensity	Perceived shaking	Damage	PGA(*g*)
I	Not felt except by a very few under especially favorable circumstances	**None**	<<0.01
II	Felt only by a few persons at rest, especially on upper floors of buildings	**None**	<0.01
III	Felt quite distinctly indoors; especially on upper floors of buildings, but many people do not recognize it as an earthquake	**None**	<0.01
IV	During the day felt indoors by many, outdoors by few. At night some awakened	**None**	0.01–0.04
V	Felt by nearly everyone, many awakened	**Very light** — Some dishes and windows. broken; cracked plaster in a few places; unstable objects overturned	0.04-0.09
VI	Felt by all, many frightened	**Light** — Some heavy furniture moved; a few instances of fallen plaster and damaged chimneys	0.09–0.18
VII	Very strong	**Moderate** — Damage negligible in buildings of good design and construction; slight to moderate in well-built ordinary structures; considerable in poorly built or badly designed structures; some chimneys broken	0.18–0.34
VIII	Severe — Persons driving cars disturbed	**Moderate to heavy** — Damage slight in specially designed structures; considerable in ordinary substantial buildings, with partial collapse; great in poorly built structures; chimneys toppled	0.34–0.65
IX	Violent	**Heavy** — Damage considerable in specially designed structures; well-designed frame structures thrown out of plumb; great in substantial buildings, with partial collapse. Buildings shifted off foundations	0.65–1.24
X	Extreme	**Very heavy** — Some well-built wooden structures destroyed; most masonry and frame structures destroyed with foundations	>1.24
XI	Extreme	**Extreme** — Few, if any, (masonry) structures remain standing	>1.24
XII	Extreme	**Extreme** — Damage total	>1.24

River and in localized areas of thick Qff deposits in areas east of the Willamette River and the Tualatin basin (Sheet 5).

500-year probabilistic maps

The probabilistic ground motions at a return period of 500 years are shown on Sheets 6, 7, and 8. A comparison of the rock peak accelerations computed in this study with larger scale maps developed by Geomatrix Consultants (1995) for the entire state and by the U.S. Geological Survey for the nation (Frankel and others, 1996) indicates our values are higher by at least 50 percent. There are three factors for this increase in the calculated hazard in the Portland metropolitan area that were not considered in the two previous studies: (1) the Oatfield, East Bank, and Mollala-Canby faults were not included in the previous studies; (2) the Portland Hills fault was assigned a higher slip rate—by a factor of two; and (3) a greater weight was given to the occurrence of the M_W 9.0 Cascadia subduction zone earthquake.

Site amplification at peak horizontal acceleration does not vary significantly in the metropolitan area at these ground motion levels (Sheet 6). The highest peak values are in the Portland Hills because of the contributions to

the probabilistic hazard from the Portland Hills and Oatfield faults. At 0.2-second spectral acceleration, site amplification is more evident particularly in the Portland Hills and damping is more prominent along the Columbia River (Sheet 7). Similar to the other 1.0-second spectral acceleration maps, the highest values are east of the Willamette River and along the Columbia River (Sheet 8).

2,500-year probabilistic maps

As expected, the probabilistic peak horizontal accelerations are higher at a 2,500-year return period (Sheet 9). At moderate- to high-input rock motions, site amplification is relatively significant as depicted in the highest levels in the Portland Hills. The hazard contributions of the Portland Hills and Oatfield faults are also illustrated on the map. Damping of high-frequency ground shaking by the thick Qal deposits along the Columbia River is a significant feature of the map.

Similarly, at 0.2-second spectral acceleration, site amplification and damping are quite pronounced due to the variable nature of deposits in the Portland area (Sheet 10). The pattern exhibited on Sheet 11 for 1.0-second spectral acceleration is similar to the other long-period hazard maps.

SUMMARY

The purpose of this study was to quantify the earthquake ground shaking that might be experienced in the Portland metropolitan area in terms of both possible events and probabilities. From either perspective, the Portland metropolitan area will be subjected to earthquake ground shaking stronger than ever experienced in historical times. In retrospect, given Portland's location above a seismically active, albeit at present quiescent, plate boundary, such predicted strong ground motions are not surprising.

The most severe ground shaking in Portland will be the result of a large earthquake on any one of several local faults as exemplified by the Portland Hills fault M_W 6.8 scenario map. The high ground motions, which will be generated by this scenario (peak horizontal acceleration >0.5 *g*), have return periods of about 2,000 to 10,000 years, based on the probabilistic analysis. In the Portland Hills fault scenario, ground shaking will be enhanced in areas in the hanging wall of the fault such as the Portland Hills. A M_W 9.0 earthquake along the megathrust of the Cascadia subduction zone will generate damaging ground motions particularly at long periods (e.g., 1.0-second spectral acceleration).

Probabilistic ground motions on rock computed in this study, though not displayed on the maps, are higher than previously estimated, because earlier analyses did not incorporate recent data on local crustal faults and the Cascadia subduction zone. The 500- and 2,500-year return period maps, which incorporate the effects of surficial deposits, display strong ground motion levels that are significant to engineering design.

It is evident that the presence of unconsolidated sediments can significantly influence ground motions in Portland. Both site amplification as large as a factor of two, or damping (reduction by 50 percent), will alter ground shaking relative to the top of the Columbia River basalt, depending on spectral frequency and the level of the rock ground motions. The contrast between the high-velocity basalt and the low-velocity sedimentary deposits is a major factor in site amplification. High-frequency site amplification can be particularly large in the Portland Hills. In contrast, damping of high-frequency ground motions will be prevalent along the Columbia River, where thick Qal deposits will amplify long-period ground motions. Finally, the presence of Columbia River basalt, which does not significantly dampen out high-frequency ground motions, compared to typical nonigneous rock in the western United States, will further enhance earthquake ground shaking in the Portland metropolitan area.

ACKNOWLEDGMENTS

This study was funded by the U.S. Geological Survey under Award 1434-HQ-96-GR-02727. Financial assistance for the publication of these maps was also provided by DOGAMI and the Professional Development Fund of URS Greiner Woodward Clyde Federal Services. We gratefully acknowledge their support. We would like to thank the many individuals who provided data, information, and assistance, including Silvio Pezzopane, Rick Blakely, Ray Wells, Tom Pratt, Ian

Madin, Brian Atwater, Tim Walsh, Sam Johnson, Art Frankel, Jerry Black, Zhenming Wang, and Bob Youngs. Special thanks to Craig Weaver and John Beaulieu for their strong support of our efforts and Sam Maley, Fumiko Goss, Jewel Clay, Lou Clark, and Paul Staub for assisting in the preparation of this publication. The maps and report benefited from reviews by Bill Elliott, Michael Hagerty, David Driscoll, Willard Titus, and David Bugni.

REFERENCES CITED

Abrahamson, N.A., and Shedlock, K.M., 1997, Overview [special issue on ground motion attenuation]: Seismological Research Letters, v. 68, no. 1, p. 9–23.

Abrahamson, N.A., and Silva, W.J., 1997, Empirical response spectral attenuation relations for shallow crustal earthquakes: Seismological Research Letters, v. 68, p. 94–127.

Atkinson, G.M., 1995, Attenuation and source parameters of earthquakes in the Cascadia region: Seismological Society of America Bulletin, v. 85, no. 5, p. 1327–1342.

Atwater, B.F., Nelson, A.R., Clague, J.J., Carver, G.A., Yamaguchi, D.K., Bobrowsky, P.T., Bourgeois, J., Darienzo, M.E., Grant, W.C., Hemphill-Haley, E., Kelsey, H.M. Jacoby, G.C., Nishenko, S.P., Palmer, S.P., Peterson, C.D., and Reinhart, M.A., 1995, Summary of coastal geologic evidence for past great earthquakes at the Cascadia subduction zone: Earthquake Spectra, v. 11, no. 1, p. 1–18.

Beeson, M.H., Tolan, T.L., and Madin, I.P., 1991, Geologic map of the Portland quadrangle, Multnomah and Washington Counties, Oregon, and Clark County, Washington: Oregon Department of Geology and Mineral Industries Geological Map Series GMS–75, scale 1:24,000.

Blakely, R.J., Wells, R.E., Yelin, T.S., Madin, I.P., and Beeson, M.H., 1995, Tectonic setting of the Portland-Vancouver area, Oregon and Washington: Constraints from low-altitude aeromagnetic data: Geological Society of America Bulletin, v. 107, no. 9, p. 1051–1062.

Boore, D.M., Joyner, W.B., and Fumal, T.E., 1997, Equations for estimating horizontal response spectra and peak acceleration from western North American earthquakes: A summary of recent work: Seismological Research Letters, v. 68, p. 128–153.

Bott, J.D.J., and Wong, I.G., 1993, Historical earthquakes in and around Portland, Oregon: Oregon Geology, v. 55, no. 5, p. 116–122.

Campbell, K.W., 1997, Empirical near-source attenuation relationships for horizontal and vertical components of peak ground acceleration, peak ground velocity, and pseudo-absolute acceleration response spectra: Seismological Research Letters, v. 68, p. 154–179.

Cohee, B.P., Somerville, P.G., and Abrahamson, N.A., 1991, Simulated ground motions for hypothesized M_w = 8 subduction earthquakes in Washington and Oregon: Seismological Society of America Bulletin, v. 81, p. 28–56.

Frankel, A., 1995, Mapping seismic hazard in the central and eastern United States: Seismological Research Letters, v. 66, p. 8–21.

Frankel, A., Mueller, C., Barnard, T., Perkins, D., Leyendecker, E.V., Dickman, N., Hanson, S., and Hopper, M., 1996, National seismic-hazard maps; documentation June 1996: U.S. Geological Survey Open-File Report 96–532, 110 p.

Geomatrix Consultants, 1995, Seismic design mapping, State of Oregon: Final report to Oregon Department of Transportation, Project no. 2442, var. pag.

Goldfinger, C., McCaffrey, R., Murray, M., Zwick, P., Nabelek, J., Smith, C.L., and Johnson, C., 1999, GPS constraints on plate coupling in central western Oregon [abs.]: Seismological Research Letters, v. 70, p. 244–245.

Hyndman, R.D., and Wang, K., 1995, The rupture zone of Cascadia great earthquakes from current deformation and the thermal regime: Journal of Geophysical Research, v. 100, p. 22, 133–22, 154.

Ludwin, R.S., Weaver, C.S., and Crosson, R.S., 1991 Seismicity of Washington and Oregon, chap. 6 *of* Slemmons, D.B., Engdahl, E.R., Zoback, M., and Blackwell, D., eds., Neotectonics of North America: Boulder, Colo., Geological Society of America Decade of North American Geology, Decade Map Volume 1, p. 77–98.

Mabey, M.A., and Madin, I.P., 1993, Ground motion amplification map, Portland quadrangle, Oregon, *in* Mabey, M.A., Madin, I.P., Youd, T.L., Jones, C.F., 1993, Earthquake hazard maps of the Portland quadrangle, Multnomah and Washington Counties, Oregon, and Clark County, Washington: Oregon Department of Geology and Mineral Industries Geological Map Series GMS-79, Plate 2, 1:24,000.

Madin, I.P., 1990, Earthquake-hazard geology maps of the Portland metropolitan area, Oregon: Oregon Department of Geology and Mineral Industries Open-File Report O–90–2, 21 p., 8 maps, 1:24,000.

Peterson, C.D., and Darienzo, M.E., 1996, Discrimination of climatic, oceanic, and tectonic mechanisms of cyclic marsh burial, Alsea Bay, Oregon, *in* Rogers, A.M., Walsh, T.J., Kockelman, W.J., and Priest, G.R., eds., Assessing earthquake hazards and reducing risk in the Pacific Northwest: U.S. Geological Survey Professional Paper 1560, v. 1, p. 115–146.

Pezzopane, S.K. 1993. Active faults and earthquake ground motions in Oregon: Eugene, Oreg., University of Oregon doctoral dissertation, 208 p.

Pratt, T.L, Odum, J., Stephenson, W., Williams, R., Dadisman, S., Holmes, M., and Haug, B., in preparation, Late Pleistocene and Holocene tectonics of the Portland basin, Oregon and Washington, from high-resolution seismic profiling: Submitted to Seismological Society of America Bulletin.

Sadigh, K., Chang, C.-Y., Egan, J.A., Makdisi, F., and Youngs, R.R., 1997, Attenuation relationships for shallow crustal earthquakes based on California strong motion data: Seismological Research Letters, v. 68, p. 180–189.

Satake, K., Shimazaki, K., Tsuji, Y., and Ueda, K., 1996, Time and size of a giant earthquake in Cascadia inferred from Japanese tsunami records of January 1700: Nature, v. 379, p. 246–249.

Silva, W.J., Abrahamson, N., Toro, G., and Costantino, C., 1997, Description and validation of the stochastic ground motion model: Unpublished report prepared for Brookhaven National Laboratory, Associated Universities, Inc.

Silva, W.J., and Darragh, R.B., 1993, Engineering characterization of strong ground motion recorded at rock sites: Unpublished report submitted to Electric Power Research Institute, Research Project RP 2556–48.

Silva, W.J., Wong, I.G., and Darragh, R.B., 1998, Engineering characterization of earthquake strong ground motions in the Pacific Northwest, *in* Rogers, A.M., Walsh, T.J., Kockelman, W.J., and Priest, G.R., eds., Assessing earthquake hazards and reducing risk in the Pacific Northwest: U.S. Geological Survey Professional Paper 1560, v. 2, p. 313–324.

Stanley, W.D., Johnson, S.Y., Qamar, A.I., Weaver, C.S., and Williams, J.M., 1996, Tectonics and seismicity of the southern Washington Cascade Range: Seismological Society of America Bulletin, v. 86, p. 1–18.

Trehu, A.M., Asudeh, I., Brocher, T.M., Luetgert, J.H., Mooney, W.D., Nabelek, J.L., and Nakamura, Y., 1994, Crustal architecture of the Cascadia forearc: Science, v. 266, p. 237–242.

Wald, D.J., Quitoriano, V., Heaton, T.H., and Kanomori, H., 1999, Relationships between peak ground acceleration, peak ground velocity, and Modified Mercalli intensity in California: Earthquake Spectra, v. 15, p. 557–564.

Weaver, C.S., and Smith, S.W., 1983, Regional tectonic and earthquake hazard implications of a crustal fault zone in southwestern Washington: Journal of Geophysical Research, v. 88, p. 10,371–10,383.

Wells, D.L., and Coppersmith, K.J., 1994, New empirical relationships among magnitude, rupture length, rupture width, and surface displacement: Seismological Society of America Bulletin, v. 84, no. 4, p. 974–1002.

Wells, R.E., Weaver, C.S., and Blakely, R.J., 1998, Forearc migration in Cascadia and its neotectonic significance: Geology, v. 26, no. 8, p. 759–762.

Wesnousky, S.G., 1986, Quaternary faults and seismic hazards in California: Journal of Geophysical Research, v. 91, p. 12,587–12,632.

Wong, I.G., 1997, The historical earthquake record in the Pacific Northwest: Applications and implications to seismic hazard assessment, *in* Wang, Y., and Neuendorf, K.K.E., eds., Earthquakes—Converging at Cascadia: Oregon Department of Geology and Mineral Industries Special Paper 28/Association of Engineering Geologists Special Publication 10, p. 19–36.

Wong, I., Bott, J., Silva, W., Anderson, D., Mabey, M., Metcalfe, B., Olig, S., Sanford, A., Lin, K-W., Wright, D., and Sojourner, A., 1998, Microzoning for earthquake ground shaking in three urban areas in the western United States: Earthquake Engineering Research Institute, Sixth National Conference on Earthquake Engineering Proceedings, CD-ROM.

Wong, I.G., Pezzopane, S.K., and Blakely, R., 1999, A characterization of seismic sources in western Washington and northwestern Oregon [abs.]: Seismological Research Letters, v. 70, no. 2, p. 221.

Wong, I.G., and Silva, W.J., 1998, Earthquake ground shaking hazards in the Portland and Seattle metropolitan areas, *in* Dakoulas, P., Yegian, M., and Holtz, R.D., eds., Geotechnical earthquake engineering and soil dynamics III: American Society of Civil Engineers Geotechnical Special Publication 75, v. 1, p. 66–78.

Wong, I.G., Silva, W.J., Youngs, R.R., and Stark, C.L., 1996, Numerical earthquake ground motion modeling and its use in microzonation: Pergamon Press, 11th World Conference on Earthquake Engineering Proceedings, CD-ROM.

Youngs, R.R., Chiou, S.-J, Silva, W.J., and Humphrey, J.R., 1997, Strong ground motion attenuation relationships for subduction zone earthquakes: Seismological Research Letters, v. 68, p. 5873.

Youngs, R.R., and Coppersmith, K.J., 1985, Implications of fault slip rates and earthquake recurrence models to probabilistic seismic hazard estimates: Seismological Society of America Bulletin, v. 75, p. 939–964.